Nanoscale

COMMUNICATION

View Article Online
View Journal | View Issue



Cite this: *Nanoscale*, 2014, **6**, 13451

Received 23rd July 2014,
Accepted 23rd September 2014

DOI: 10.1039/c4nr04164j

www.rsc.org/nanoscale

# siRNA liposome-gold nanorod vectors for multispectral optoacoustic tomography theranostics†

Adrian Taruttis,[a,b] Neus Lozano,[c] Antonio Nunes,[b] Dhifaf A. Jasim,[c] Nicolas Beziere,[a,b] Eva Herzog,[a,b] Kostas Kostarelos*[c] and Vasilis Ntziachristos*[a,b]

**Therapeutic applications of gene silencing using siRNA have seen increasing interest over the past decade. The optimization of the delivery and biodistribution of siRNA using liposome-gold nanorod (AuNRs) nanoscale carriers can greatly benefit from adept imaging methods that can visualize the time-resolved delivery performance of such vectors. In this work, we describe the effect of AuNR length incorporated with liposomes and show their complexation with siRNA as a novel gene delivery vehicle. We demonstrate the application of multispectral optoacoustic tomography (MSOT) to longitudinally visualize the localisation of siRNA carrying liposome-AuNR hybrids within tumors. Combination of *in vivo* MSOT with *ex vivo* fluorescence cryo-slice imaging offers further insight into the siRNA transport and activity obtained.**

The promise of therapeutic applications of small interfering RNA (siRNA) has raised interest in their use for prevention and treatment of a variety of diseases, including cancer. Routine clinical use of siRNA therapeutics will depend in particular on the development of appropriate delivery vehicles.[1] Naked siRNAs are degraded by enzymes *in vivo*, are not suited for crossing cell membranes, and may not have suitable pharmacokinetic profiles for successfully reaching their targets after administration. It is therefore the task of the delivery vehicle to protect the siRNA from the biological environment and safely carry it to its specific target.

Liposomes are considered among the most promising delivery vehicles for siRNA, due to their history as vehicles for chemotherapeutic agents,[2] their fusogenic capacity[3] and the wide range of chemical modifications possible to tailor both their targeting and release profiles.[4] Cationic liposomes are widely used as transfection agents because they are able to form complexes with negatively charged siRNA *via* electrostatic interactions. Specifically, liposomes consisting of the cationic lipid DOTAP and cholesterol and also the incorporation of DSPE-PEG as a steric stabilizer have been previously studied, using mixing and encapsulation protocols for generating liposome/siRNA complexes.[5]

*In vivo* imaging can become an essential method for optimizing siRNA delivery vehicles by monitoring their pharmacokinetic and biodistribution profiles. Requirements for a suitable imaging modality include the ability to non-invasively resolve the distribution of the nanocarriers at sufficient spatial resolution throughout relevant animal models of disease and enable longitudinal studies at adequate temporal resolution. Multispectral optoacoustic tomography (MSOT) offers ideal characteristics for sensing nanoparticles and elucidating their distribution profile. The method is based on optoacoustics, *i.e.* the generation of acoustic waves after absorption of light pulses in the nanosecond range by tissue absorbers. The method is therefore unique in that it can visualize optical absorption deep inside tissue (at least 2 cm) with resolutions limited by ultrasonic diffraction. By capitalizing on multispectral detection, MSOT can identify the spectral signatures of different photo-absorbing molecules. This feature can be applied, for example, in resolving oxy- and deoxyhemoglobin or distinguishing extrinsically administered agents labeled with organic dyes or gold or carbon nanoparticles from tissue background absorption.[6–10] In addition, visualization of optical contrast in real-time can be achieved, which is valuable in resolving fast kinetic profiles of injected agents.[11]

Gold nanorods (AuNRs) provide high optical absorption with a peak that can be tuned by adjusting the particle dimensions. AuNRs have been demonstrated as effective optoacoustic contrast agents in a number of studies.[12–15] While other gold nanoparticles have been investigated for optoacoustic imaging, including nanohexapods, nanocages[16] and nanoshells,[17] they are not as widely established or available, do not offer as narrow size distribution as AuNRs and have not been shown to incorporate stably onto lipid bilayers. Alternative to gold

[a]*Chair for Biological Imaging, Technische Universität München, Ismaningerstr. 22, 81675 München, Germany. E-mail: v.ntziachristos@tum.de*
[b]*Institute for Biological and Medical Imaging, Helmholtz Zentrum München, Ingolstädter Landstr. 1, 85764 Neuherberg, Germany*
[c]*Nanomedicine Laboratory, Faculty of Medical & Human Sciences, The University of Manchester, Manchester M13 9PT, UK. E-mail: kostas.kostarelos@manchester.ac.uk*

†Electronic supplementary information (ESI) available: Experimental section and dark-field microscopy in both tumors 24 h after injection of the complex have been included. See DOI: 10.1039/c4nr04164j

nanoparticles could involve organic absorbers, such as phospholipid–porphyrin conjugates that have been investigated for liposome-like structures in this context.[18]

We prepared liposome-AuNR hybrids[19] with optimized-length AuNRs to allow these nanocarriers to be resolved by MSOT imaging. In addition, the liposomes were labeled with NIR-797 fluorescent tag to allow their validation using fluorescence cryoslicing imaging (FCSI) as a standard of reference. We were able to resolve the liposome-AuNR hybrids *in vivo* with patterns that matched our validation using fluorescence-based signal, showing that MSOT can perfectly resolve the NIR-liposome-AuNR hybrids carrying siRNA *in vivo*. Moreover, we demonstrated the biological effect of the hybrids carrying siPLK1 using TUNEL Assay.

Fig. 1 shows the optical properties of three different lengths of AuNRs (29 nm – $AuNR_{700}$, 38 nm – $AuNR_{780}$ and 45 nm – $AuNR_{850}$) and their hybrids formed with cationic labeled liposomes (NIR797-DOPE)-DOTAP : Chol (NIR-liposome). The absorbance spectra for the hybrids with $AuNR_{700}$ and $AuNR_{850}$ do not show a significant deviation in the wavelength in comparison to the AuNR alone, while the wavelength significantly shifts from 780 to 792 nm for the $hybrid_{780}$. This red shift of 12 nm for the NIR-liposome-$AuNR_{780}$ hybrids confirms the interaction between liposomes and $AuNR_{780}$ but this interaction is not observed for the shorter and longer AuNR studied. Furthermore, the interaction between liposomes and $AuNR_{780}$ induces a 2-fold increase on the absorbance compared to AuNR alone that evidences an enhancement of the stability of the AuNR.[20] Because of the higher absorption intensity will lead the better MSOT resolution the liposomes with $AuNR_{780}$ have been selected for the experiments detailed below.

We continued by exploring the interaction of the NIR-liposome-$AuNR_{780}$ hybrids with scramble siRNA as a potential theranostic agent. Agarose gel electrophoresis was performed for $AuNR_{780}$ (used as a control), NIR-liposomes (L) and NIR-liposome-$AuNR_{780}$ hybrids (H) to study the extent of association of the cationic liposomes with siRNA, as shown in Fig. 2A. As expected, the $AuNR_{780}$ alone do not interact with the negative siRNA (top panel) because of the slightly negatively charged of the AuNRs. For plain cationic liposomes (L) and for the hybrids (H), the charge ratio required for the total siRNA complexation is 3 and 2, respectively. Further studies should be carried out to understand the slight improvement on the complexation for the hybrids compared to the liposomes alone. It can be concluded that the presence of AuNR in the liposomes does not prevent the siRNA complexation. These findings suggest the NIR-liposome-$AuNR_{780}$ hybrid as a promising novel candidate vector for gene delivery. The hydrodynamic diameter and ζ-potential values of the NIR-liposome-$AuNR_{780}$ hybrids were plotted as a function of the charge ratio ($N/P$), as shown in Fig. 2B and 2C. The particle size shows an increase near the isoelectric point ($N/P \sim 1:1$) at the same time that the ζ–potential is ranged between −15 and 15 mV where the charge is neutralized. To confirm the presence of AuNR after the complexation with siRNA, TEM was performed

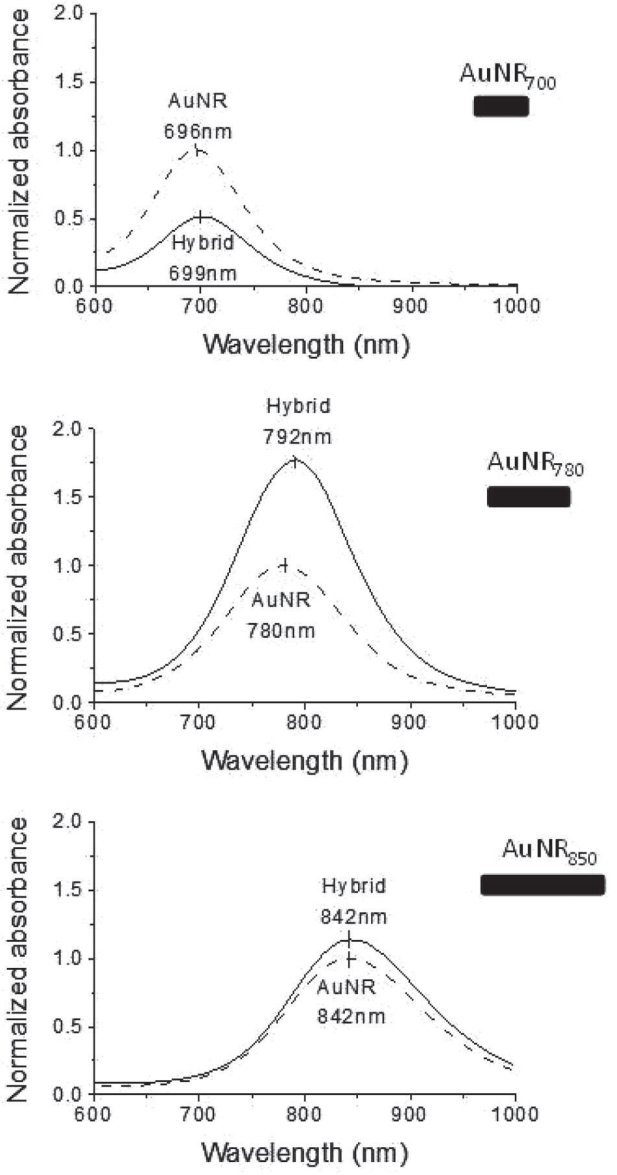


**Fig. 1** UV-Vis absorption spectra normalized for AuNR alone (dashed lines) and NIR-liposome-AuNR hybrids (solid lines) at different lengths of AuNR: 29 nm ($AuNR_{700}$), 38 nm ($AuNR_{780}$) and 45 nm ($AuNR_{850}$). Axial size of 10 nm.

(Fig. 2D). Effectively, the NIR-liposome-$AuNR_{780}$/siRNA complexes display AuNR in the liposomes, corroborating the strong interaction between AuNR and liposomes.

An advantageous strategy for visualizing the delivery of the liposomal vectors is to employ MSOT resolving their strong absorption in the NIR region. Fig. 3 shows the schematic of the NIR-liposome-$AuNR_{780}$/siRNA complexes formulated and the comparative graph of the absorption spectrum (dotted line) *versus* optoacoustic signal (crosses) from complex-containing phantom inclusion confirming that the optoacoustic signal amplitude is proportional to the amount of energy absorbed per wavelength. The results suggest that MSOT can detect the hybrids and resolve their absorption

 

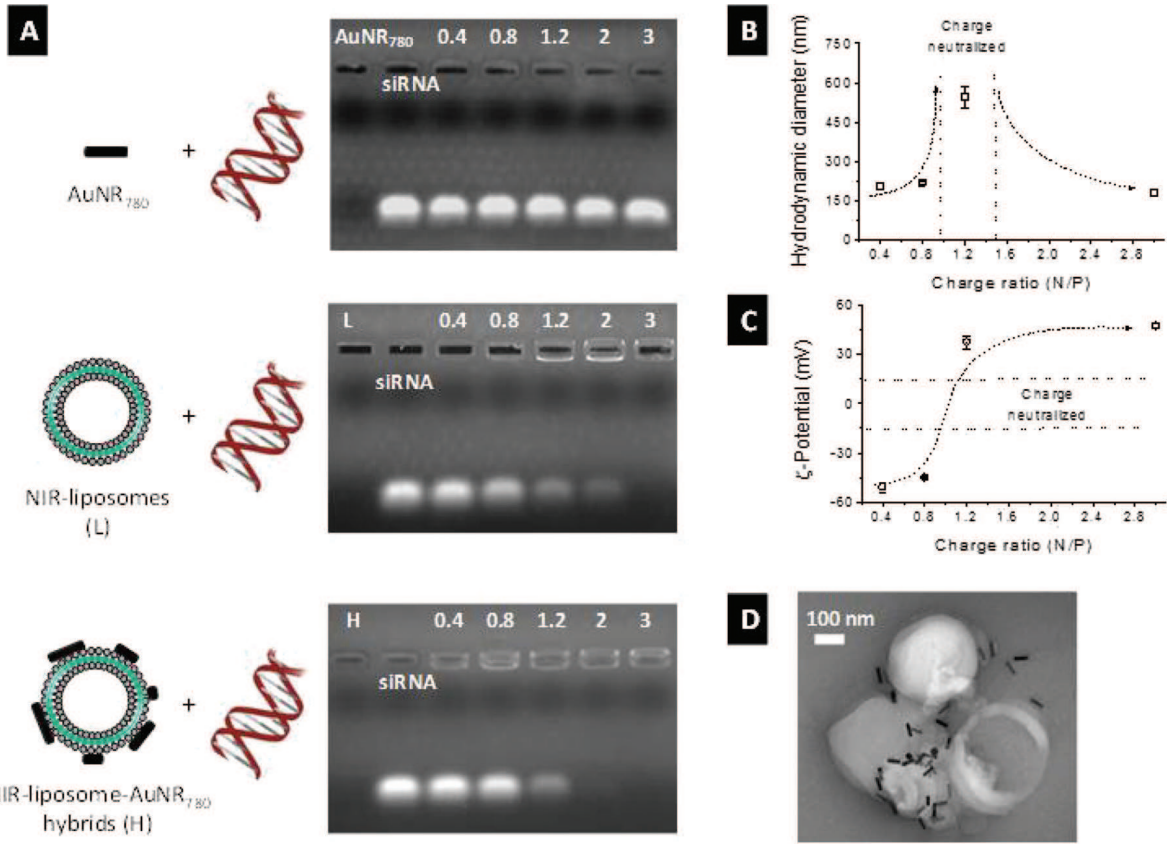


**Fig. 2** (A) Schematic of $AuNR_{780}$, NIR-liposomes (L) and NIR-liposome-$AuNR_{780}$ hybrids (H) with siRNA and their complexation studies with siRNA. Agarose gel electrophoresis at charge ratios (*N*/*P*, positively charged nitrogen to negatively charged phosphate) from 0.4 to 3 and incubated for 30 min at room temperature before loading onto 1% agarose/TBE gel. *N*/*P* calculated for fixed siRNA concentration of 0.5 μg. (B) Hydrodynamic diameter and (C) ζ-potential for NIR-liposome-$AuNR_{780}$/siRNA complexes at different charge ratios (*N*/*P*). (D) TEM micrograph for the hybrid/siRNA complexes at *N*/*P* of 0.8.

spectrum, which is the means by which the liposomes could be identified in tissues in the presence of background absorption.

*In vivo* experiments were performed to confirm MSOT imaging of liposome vectors using 4T1 and HT29 tumor models. MSOT was employed to image both tumor models before injection, 10 min and 24 h after intratumoral injection of the NIR-liposome-$AuNR_{780}$ hybrids complexed with the apoptotic siPLK1 (Fig. 4A). At single wavelength MSOT provides images of anatomic information regarding the tumor mass and vasculature based on the endogenous optical absorption of tissues. In contrast to implementations focused on visualizing primarily blood vessels, MSOT offers a more complete picture of anatomical structures in the animal, primarily due to the use of accurate model-based inversion methods and the operation at the near-infrared. Using then spectral differentiation, the specific optoacoustic signature of AuNR was identified after injection (10 min time point), as illustrated by the green color overlap. Both tumour models were imaged again at 4 hour (data not shown) and 24 h post-injection. We could observe that the injected dose remained stable in the site of injection after 24 h, protecting siRNA clearance from the tumor and therefore enabling apotosis.

Validation of the spatial liposome distribution in 4T1 and HT29 tumors was performed by fluorescence cryoslicing imaging (FCSI) 24 h after injection (Fig. 4B). Liposome detection by FCSI was based on the NIR-797 fluorescent tag and demonstrated excellent congruence with the MSOT images. These findings infer that despite the complexation of the therapeutic agent siPLK1, our delivery system (NIR-liposome-AuNR) remains stable *in vivo* 24 h after intratumoral injection, in analogy to the stability observed without the therapeutic agent.[19] Dark-field scattering microscopy images of tissue slices from the tumors 24 h after injection reveal AuNRs in the regions identified by MSOT, serving as further validation (Fig. S1 – ESI†).

The biological activity of siPLK1 in 4T1 and HT29 tumors was validated by TUNEL assay (Fig. 5). Over time, for both tumor models, the GFP signal becomes brighter indicating an increased induction of apoptosis. 24 h after intratumoral injection, a strong signal could be visualized within an extensive volume, suggesting the diffusion of apoptosis throughout the tumor mass. Overall, the HT29 model appeared to be more sensitive to NIR-liposome-$AuNR_{780}$ nanocarrier, as the initial apoptosis values (at 10 min) were slightly higher compared to 4T1 model.

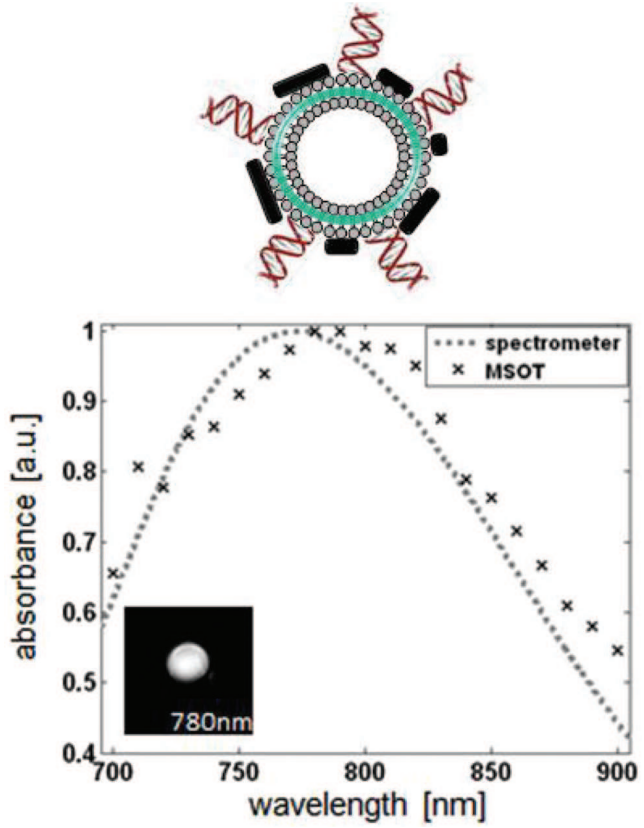


**Fig. 3** Schematic of the NIR-liposome-AuNR$_{780}$/siRNA complexes and comparative graph for the absorption spectrum of the complex measured in a spectrometer (dotted line) *versus* the amplitude of MSOT signal from complex-containing phantom inclusion (crosses) plotted against wavelength. Inset: optoacoustic image of phantom inclusion at 780 nm excitation.

Our experimental results prove the complexation of the therapeutic agent siRNA in the liposome-AuNR hybrids and also demonstrate *in vivo* MSOT imaging that resolves the liposome-AuNR$_{780}$ hybrids as potential nanocarriers of siRNA delivery within subcutaneous tumors in mice. The successful MSOT detection of this delivery system was validated by FCSI imaging and darkfield microscopy in two different cancer cell lines. These images provided by MSOT reproduced the spatial distribution of the nanocarriers within tumors with a higher accuracy (spatial resolution) compared to conventional optical imaging approaches. Overall, further MSOT virtues are observed in the studies. First, the ability to provide high-resolution anatomical optical contrast and accurate co-registration of liposome signals enables accurate orientation of the liposome presence relative to the tumor and the rest of the animal. Second, the liposomes were resolved not as signal changes over baseline but based on their absorption spectral signature. Spectral detection distinguishes nanoparticles over background absorption without requiring baseline measurements. Therefore imaging over long periods of time can be accomplished. Longitudinal observations enabled herein the conclusion that the liposomes exhibited minimal diffusion through the tumor volume over 24 hours, independent of the cancer cell line used.

While optical microscopy offers high-resolution imaging of labeled particles, it can only achieve depths in the range of tens to hundreds of microns,[21] making it unsuitable for revealing biodistribution *in vivo*. Optical microscopy methods such as near infrared fluorescence (NIRF), are limited by strong photon diffusion, which conceals information on deep tissue biodistribution and processes.[21] Nuclear imaging modalities are highly valuable in biodistribution studies but do not typically display spatial resolutions appropriate for identifying small features.[22] Their use of ionizing radiation may also complicate experimental procedures and isotope decay can hinder longitudinal studies depending on the label employed. Conversely, high resolution radiological approaches such as Magnetic Resonance Imaging (MRI), X-ray CT and ultrasound lack sensitivity to molecular contrast.

Our study indicated that MSOT can play a role in preclinical imaging of nucleic acid delivery, or more specifically, the potential use of liposome-AuNR hybrids for delivery of siRNA. Besides the unique optical absorption contrast attained by the method, allowing sensitive detection of optically absorbing agents (AuNRs in that case), MSOT offers a number of advantages to preclinical imaging studies. First, and most significantly, the resolution does not degrade with depth as is the case with pure optical imaging techniques, allowing, in the implementation used in this study, resolutions in the range of 100–200 μm throughout an imaged mouse. This means that distributions of nanocarriers can be pinpointed throughout tumor mass and elsewhere in tissues using real-time, non-invasive observations. The multispectral nature of MSOT allows not only the specific separation of exogenous contrast from endogenous tissue absorbers, but can potentially be used to resolve multiple agents of interest simultaneously. A complete single wavelength image is acquired from each laser pulse within 40 μs. In this implementation, 10 pulses a second give rise to 10 transverse images, allowing live visualization of the animal being imaged, similar to ultrasound imaging.[23] Multispectral imaging with MSOT can be performed within 100 milliseconds or less, and it is therefore possible to specifically resolve labeled agents with a conveniently high temporal resolution. Animals can be imaged at multiple time points for longitudinal studies after the initial administration of the agents.

MSOT is capable of imaging agents that provide sufficient optical absorption, and is therefore not limited to using AuNR for contrast generation.[24] AuNR provide high optical absorption per particle, therefore enable sensitive imaging of AuNR-enhanced agents or vectors. While the NIR-797 dye used to label the liposomes for fluorescence detection could also be detected by MSOT, the amount of the dye per liposome would have to be greatly increased to produce optical absorption comparable to AuNR.

While two-dimensional images were analyzed in this study, MSOT is typically implemented for three-dimensional imaging. As a next step, the three-dimensional capabilities of

 

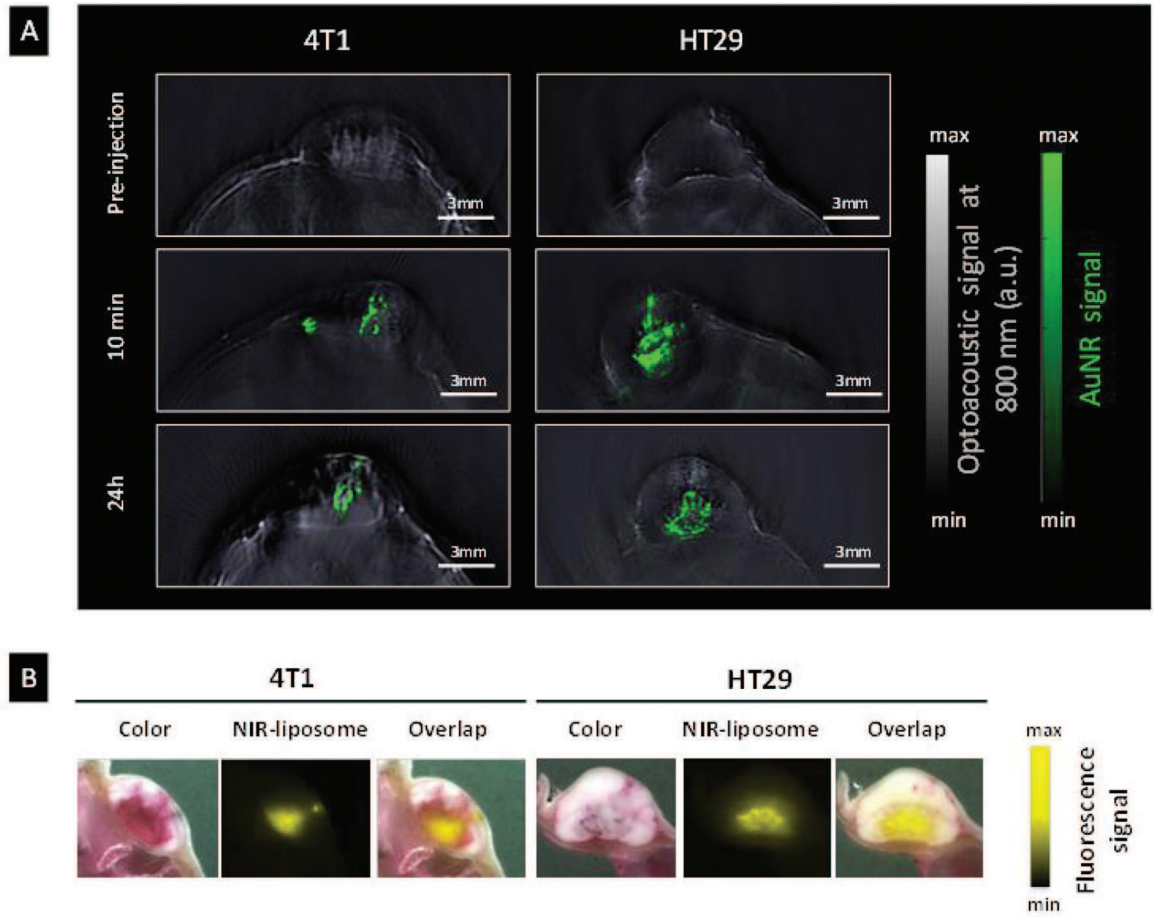


**Fig. 4** (A) *In vivo* MSOT transverse images showing multispectrally resolved NIR-liposome-AuNR$_{780}$/siPLK1 complexes (green overlay) within a 4T1 and HT29 tumors before, 10 min and 24 h after intratumoral injection. (B) Validation of NIR-liposomes (yellow signals) in 4T1 and HT29 tumors using fluorescence cryoslicing imaging (FCSI) of the corresponding cryosections taken 24 h after intratumoral injection of the NIR-liposome-AuNR$_{780}$/siPLK1 complexes.

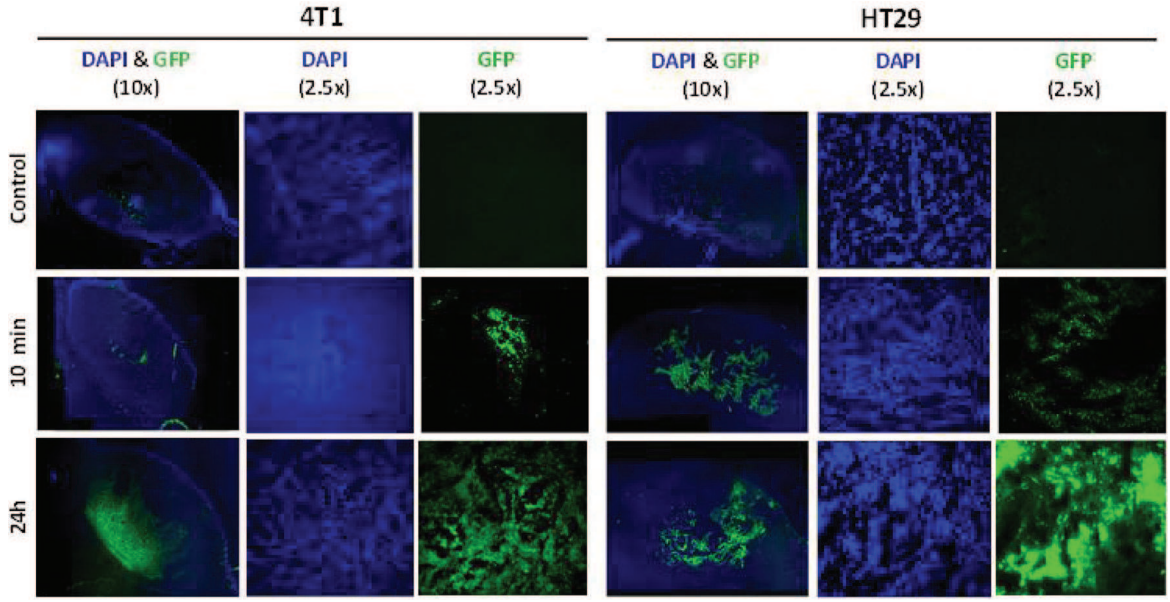


**Fig. 5** Validation of apoptosis in 4T1 and HT29 tumors using TUNEL assay at low (10×) and high (2.5×) magnification of the corresponding cryosections taken 10 min and 24 h after intratumoral injection of the NIR-liposome-AuNR$_{780}$ complexed with siPLK1. Control refers to the corresponding cryosections taken 24 h after intratumoral injection of the NIR-liposome-AuNR$_{780}$ complexed with scramble siRNA.

the system will be explored to offer better quantification of siRNA delivery systems within tissue volumes. Recently, the development of video-rate, three-dimensional systems can also allow fast three-dimensional imaging and could be particularly useful for volumetric interrogations.[25] In the future we propose utilization of liposomal theranostic systems optimized for intravenous administration, by fine tuning the release kinetics and localization *via* modification of the liposome surface functions. Additionally, we hope to tag the siRNA in such a way that it can be resolved by MSOT *in vivo* alongside the nanocarriers to achieve continuous, multi-channel imaging of its transport, tissue distribution and biological activity using a single vector system.

## Disclosures

V.N. is an equity holder in iThera Medical GmbH.

## Acknowledgements

V.N. has received funding from an Advanced Investigator Grant from the European Research Council (ERC). N.L. is partially supported by the Andalusian Initiative for Advanced Therapies promoted by the Regional Government of Andalusia, Spain. We are grateful to David McCarthy at UCL School of Pharmacy for assistance with the TEM instrumentation. The authors also wish to acknowledge Sarah Glasl for her valuable technical support on the histology and immunohistochemistry.

## References

1 K. A. Whitehead, R. Langer and D. G. Anderson, Knocking down barriers: advances in siRNA delivery, *Nat. Rev. Drug Discovery*, 2009, **8**, 129–138.
2 D. Peer, *et al.*, Nanocarriers as an emerging platform for cancer therapy, *Nat. Nanotechnol.*, 2007, **2**, 751–760.
3 M. S. Shim and Y. J. Kwon, Efficient and targeted delivery of siRNA in vivo, *FEBS J.*, 2010, **277**, 4814–4827.
4 R. R. Sawant and V. P. Torchilin, Liposomes as 'smart' pharmaceutical nanocarriers, *Soft Matter*, 2010, **6**, 4026–4044.
5 J. E. Podesta and K. Kostarelos, in *Methods Enzymol.*, ed. N. Duzgunes, Academic Press, 2009, vol. 464, pp. 343–354.
6 A. De la Zerda, *et al.*, Carbon nanotubes as photoacoustic molecular imaging agents in living mice, *Nat. Nanotechnol.*, 2008, **3**, 557–562.
7 G. P. Luke, S. Y. Nam and S. Y. Emelianov, Optical wavelength selection for improved spectroscopic photoacoustic imaging, *Photoacoustics*, 2013, **1**, 36–42.
8 J. Laufer, D. Delpy, C. Elwell and P. Beard, Quantitative spatially resolved measurement of tissue chromophore concentrations using photoacoustic spectroscopy: application to the measurement of blood oxygenation and haemoglobin concentration, *Phys. Med. Biol.*, 2007, **52**, 141–168.
9 D. Razansky, *et al.*, Multispectral opto-acoustic tomography of deep-seated fluorescent proteins in vivo, *Nat. Photonics*, 2009, **3**, 412–417.
10 Q. Zhang, *et al.*, Gold nanoparticles as a contrast agent for in vivo tumor imaging with photoacoustic tomography, *Nanotechnology*, 2009, **20**, 395102.
11 A. Taruttis, S. Morscher, N. C. Burton, D. Razansky and V. Ntziachristos, Fast multispectral optoacoustic tomography (MSOT) for dynamic imaging of pharmacokinetics and biodistribution in multiple organs, *PLoS One*, 2012, **7**, e30491.
12 M. Eghtedari, *et al.*, High sensitivity of in vivo detection of gold nanorods using a laser optoacoustic imaging system, *Nano Lett.*, 2007, **7**, 1914–1918.
13 A. Taruttis, E. Herzog, D. Razansky and V. Ntziachristos, Real-time imaging of cardiovascular dynamics and circulating gold nanorods with multispectral optoacoustic tomography, *Opt. Express*, 2010, **18**, 19592–19602.
14 J. V. Jokerst, A. J. Cole, D. Van de Sompel and S. S. Gambhir, Gold nanorods for ovarian cancer detection with photoacoustic imaging and resection guidance via Raman imaging in living mice, *ACS Nano*, 2012, **6**, 10366–10377.
15 Y.-S. Chen, *et al.*, Silica-coated gold nanorods as photoacoustic signal nanoamplifiers, *Nano Lett.*, 2011, **11**, 348–354.
16 Y. Wang, *et al.*, Comparison study of gold nanohexapods, nanorods, and nanocages for photothermal cancer treatment, *ACS Nano*, 2013, **7**, 2068–2077.
17 Y. Wang, *et al.*, Photoacoustic Tomography of a Nanoshell Contrast Agent in the in Vivo Rat Brain, *Nano Lett.*, 2004, **4**, 1689–1692.
18 J. F. Lovell, *et al.*, Porphysome nanovesicles generated by porphyrin bilayers for use as multimodal biophotonic contrast agents, *Nat. Mater.*, 2011, **10**, 324–332.
19 N. Lozano, *et al.*, Liposome-gold nanorod hybrids for high-resolution visualization deep in tissues, *J. Am. Chem. Soc.*, 2012, **134**, 13256–13258.
20 H.-C. Huang, S. Barua, D. B. Kay and K. Rege, Simultaneous enhancement of photothermal stability and gene delivery efficacy of gold nanorods using polyelectrolytes, *ACS Nano*, 2009, **3**, 2941–2952.
21 V. Ntziachristos, Going deeper than microscopy: the optical imaging frontier in biology, *Nat. Methods*, 2010, **7**, 603–614.
22 R. Weissleder, Scaling down imaging: molecular mapping of cancer in mice, *Nat. Rev. Cancer*, 2002, **2**, 11–18.
23 A. Taruttis, J. Claussen, D. Razansky and V. Ntziachristos, Motion clustering for deblurring multispectral optoacoustic tomography images of the mouse heart, *J. Biomed. Opt.*, 2012, **17**, 016009.
24 V. Ntziachristos and D. Razansky, Molecular imaging by means of multispectral optoacoustic tomography (MSOT), *Chem. Rev.*, 2010, **110**, 2783–2794.
25 X. L. Dean-Ben, A. Ozbek and D. Razansky, Volumetric real-time tracking of peripheral human vasculature with GPU-accelerated three-dimensional optoacoustic tomography, *IEEE Trans. Med. Imaging*, 2013, **32**, 2050–2055.

 